CSMA 2017
13ème Colloque National en Calcul des Structures
15-19 Mai 2017, Presqu'île de Giens (Var)

A Variational Visco-Hyperelastic Constitutive Model for Glassy Polymers

J.-M. C. Farias[1], L. Stainier [2], E. A. Fancello[1]

[1] *UFSC, Universidade Federal de Santa Catarina,{janmichel.farias,eduardo.fancello}@ufsc.br*
[2] *GeM (UMR 6183 CNRS / Ecole Centrale de Nantes / Universite de Nantes), laurent.stainier@ec-nantes.fr*

Abstract — Constitutive models for glassy polymers have been based on the concept of a flow resistance internal variable for over 20 years. Through investigation and implementation of these state-of-the-art models, the current authors identified a new possibility for characterizing this class of polymers, which can simplify the analysis and frame them in a well posed family of constitutive models, especially suited for using the variational constitutive update approach. A visco-hyperelastic model is proposed which results in one single equation to be solved at each time step in the constitutive incremental update. Comparison against experimental data is performed and a numerical example inside a FEM framework is given.
Mots clés — Glassy Polymers, Variational Updates , Finite Viscoelasticity.

1 Introduction

Products made of polymers are undoubtedly in our daily routine. Their behavior can exhibit strong dependence on temperature [14] , strain rate [3, 8] and pressure [15], and their properties can vary drastically if processing methods and conditions change. Among them, amorphous glassy polymers are highlighted due to their widespread applicability and manufacturing flexibility. This way, the constitutive modeling of these materials depends on the improvement of experimental and numerical methods to predict their response regarding arbitrary loading histories.

Historically, Haward and Thackray (1968) [4] attempted to model these class of polymers for a long range of strains using an unidimensional rheological model. The recent work of Holopainen (2013) [5] presents a literature survey about this topic and cites the work of Boyce, Parks and Argon (1988) [3] and the work of Anand and Ames (2006) [1] as the state of the art models currently available. Holopainen proposes a new formulation, called Extended Boyce, Parks and Argon model (EBPA) and presents some results. The models provided by Boyce, Parks and Argon (1988) [3] , Anand and Gurtin (2003)[2], Anand and Ames (2006) [1] and Holopainen (2013) [5] are all based on the concept of a flow resistance internal variable, which must be solved conjointly with the problem.

Through investigation and implementation of these state-of-the-art models, the current authors identified a new possibility for characterizing this class of polymers, which can simplify the analysis and frame them in a well posed family of constitutive models, especially suited for using the variational constitutive update approach introduced by Ortiz and Stainier (1999) [6]. In the overall treatment of constitutive models, the variational approach [6] is a mechanical mathematical cornerstone, thermodynamically consistent, which allows the inclusion of a variety of dissipative mechanisms, but retaining the main properties of a conservative model such as hyperelasticity.

2 Constitutive Modeling

2.1 Kinematics

We propose a visco-hyperelastic model based on the rheological model depicted in figure (1). The kinematic relations and hypothesis are briefly introduced next. It is assumed that the deformation gra-

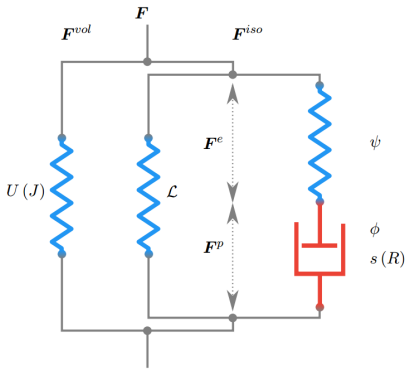

Figure 1: Rheological Model

dient $\boldsymbol{F}$ can be decomposed in an isochoric factor $\boldsymbol{F}^{iso}$ ($\det \boldsymbol{F}^{iso} = 1$) and in a volumetric factor $\boldsymbol{F}^{vol}$ ($\det \boldsymbol{F}^{vol} = J = \det \boldsymbol{F}$) as $\boldsymbol{F} = \boldsymbol{F}^{iso}\boldsymbol{F}^{vol}$.

Aiming at large strains, the multiplicative decomposition introduced by Lee (1969) is utilized to split the isochoric deformation gradient $\boldsymbol{F}^{iso}$ in two factors; an elastic deformation gradient $\boldsymbol{F}^{e}$ and an inelastic deformation gradient $\boldsymbol{F}^{p}$

$$\boldsymbol{F}^{iso} = \boldsymbol{F}^{e}\boldsymbol{F}^{p} \tag{1}$$

The same strategy is widely used in the literature and a non-exhaustive list would include [3, 2].

The inelastic flow is assumed to be isochoric, in the sense that $\det \boldsymbol{F}^{p} = 1$. As a direct consequence, the inelastic velocity gradient becomes a traceless tensor $\mathrm{tr}\boldsymbol{L}^{p} = 0$. We further assume that the flow is also irrotational, which requires the inelastic spin to be null $\boldsymbol{W}^{p} = \boldsymbol{0}$. An interesting motivation with mathematical background is presented by [2] to justify an irrotational flow assumption. Based on this condition, the inelastic velocity gradient $\boldsymbol{L}^{p}$ must be symmetric, and thus must be the same as the inelastic stretching tensor $\boldsymbol{D}^{p}$ resulting in the condition $\dot{\boldsymbol{F}}^{p} = \boldsymbol{D}^{p}\boldsymbol{F}^{p}$.

2.2 Thermodynamic Framework

The major difference among the available models used to describe glassy polymers [3, 2, 1, 5] and the current work relies on thermodynamical aspects. These previous works assume the concept of a flow resistance to be an internal variable that must be solved conjointly with the constitutive problem. Our approach does not rely on such an assumption, and thus the thermodynamic framework has to be adapted.

As stated previously, our theory is purely mechanical and based on thermodynamics. It is assumed that on a sufficiently small neighborhood around a material point, the thermodynamic state can be uniquely described by the total deformation gradient $\boldsymbol{F}$, the inelastic deformation gradient $\boldsymbol{F}^{p}$ and by a scalar quantity R named accumulated viscous strain, i.e. $\mathcal{E} = \{\boldsymbol{F}, \boldsymbol{F}^{p}, R\}$. This accumulated viscous strain is a measure of how much the material has undergone viscous stretching and is defined by

$$R = \int_0^t \sqrt{2}\,\|\boldsymbol{D}^{p}\|\,dt \tag{2}$$

In order to use the variational framework proposed by [6], it is necessary to introduce two energetic potentials: the Helmholtz free energy potential W and the dissipation potential ϕ. We assume that the Helmholtz potential can be split additively into 3 other energies

$$W(\mathcal{E}) = U(J) + \mathcal{L}\left(\boldsymbol{F}^{iso}\right) + \psi(\boldsymbol{F}, \boldsymbol{F}^{p}) \tag{3}$$

The first one is an energy based exclusively on the volumetric deformation provided by the Jacobian J. The volumetric deformation is also considered a purely elastic process, as in references [11, 12], and is given by $U(J) = \frac{\kappa}{2}(\ln J)^2$. Note that this split of a volumetric energy allows the adoption of different solution strategies, such as the variational three-field potential proposition [19] to deal with incompressibility issues.

The second energy potential comes from the eight-chain hyperelastic model introduced by [17]. This model is based on statistical mechanics and is also adopted in [2] . Note that the way it is used by [2],

i.e. as dependent on the inelastic deformation gradient, generates a back stress, while our approach does not.

Finally we consider a quadratic Hencky energy potential, given by $\psi(\varepsilon^e) = G\|\mathrm{dev}\varepsilon^e\|^2$, as dependent on the logarithmic strain from the elastic right-Cauchy tensor $\varepsilon^e = \frac{1}{2}\ln \boldsymbol{C}^e = \frac{1}{2}\ln\left(\boldsymbol{F}^{eT}\boldsymbol{F}^e\right)$.

As mentioned previously, in order to use the methodology proposed by [6] it remains necessary to define a dissipative potential. A Perzyna-like potential is adopted, as also utilized in the works of [12, 6, 9]

$$\phi\left(R,\dot{R}\right) = \begin{cases} \frac{s(R)}{m+1}\dot{R}^{m+1} & \dot{R} \geq 0 \\ \infty & \dot{R} < 0 \end{cases} \tag{4}$$

However, in [12] the dissipative potential considers a constant flow resistance s, and in [9] an elasto-visco-plastic model with linear hardening is proposed. Reference [2] does not demonstrate any dissipative potential, but a careful analysis of the flow equations reveals that analogous equations are in fact obtained by the potential (4).

When compared against other models [3, 2, 1, 5], the main difference that arises in the current formulation is the flow resistance as a state dependent variable $s(R)$, i.e., it is not solved for but rather just evaluated when needed. It is then sufficient to define an explicit function $s(R)$ that associates the material flow resistance with the accumulated viscous strain. Some examples may be useful to better understand the versatility of this function. One can consider the resistance to be constant $s(R) = s_0$ rendering a traditional Perzyna flow-rule [9, 6], or by assuming a linear dependence on the viscous rate $(m = 1)$ obtain a Newtonian flow. However, these assumptions are not satisfactory to deal with glassy polymers, as they generally show a loss of resistance in the flow mechanisms. A better choice would be a function which accounts for the possibility of a flow resistance transition, ranging from an initial state s_0 to a saturated value s_∞. This can be accomplished by the function

$$s(R) = s_\infty + (s_0 - s_\infty)\, e^{-\zeta R} \tag{5}$$

which, by the way, captures the essence of the model introduced by Boyce , Parks , Argon [3]. On the other hand, an even more elaborated choice could be the function

$$s(R) = s_\infty + e^{-\zeta R}\left[(s_0 - s_\infty)\cosh(\beta R) + \gamma \sinh(\beta R)\right] \tag{6}$$

which can deal with a peak resistance followed by a continuous loss of resistance until a saturated value is achieved. This type of relation allows a better description of the phenomena and is in consonance with the model introduced by Anand and Gurtin [2].

2.3 Constitutive Variational Problem

As the accumulated viscous strain R and its rate $\dot{R}$ are frequently addressed, it becomes convenient to perform a decomposition of the inelastic stretching tensor $\boldsymbol{D}^p$. It is assumed that this tensor can be decomposed $\boldsymbol{D}^p = \dot{R}\boldsymbol{N}$ in a positive scalar quantity $\dot{R} \in \mathbb{R}_+$and a tensor $\boldsymbol{N}$ with constrained magnitude

$$\boldsymbol{N} \in \mathcal{N} = \left\{ \boldsymbol{A} \in Sym \,|\, \mathrm{tr}\boldsymbol{A} = 0 \quad and \quad \|\boldsymbol{D}^p\| = \frac{1}{\sqrt{2}} \right\}. \tag{7}$$

This type of decomposition is often referred as an amplitude-direction decomposition, as the stretching magnitude is described by $\dot{R}$ while all the tensorial properties are held by $\boldsymbol{N}$. The constraints (7) over $\boldsymbol{N}$ arise from the constraints shared by $\boldsymbol{L}^p$, which are the symmetry and traceless conditions. By doing so, the inelastic deformation gradient rate becomes

$$\dot{\boldsymbol{F}}^p = \dot{R}\boldsymbol{N}\boldsymbol{F}^p. \tag{8}$$

This alternative approach, with the amplitude-direction assumption, is often stated as the parametrized constitutive problem [6]. To demonstrate the variational nature of the constitutive problem, still considering a continuous time description, all required equations are shown to be obtained from the stationarity conditions of a potential. It can be formally done by the statement:

Variational Principle Given a state $\mathcal{E} = \{\boldsymbol{F}, \boldsymbol{F}^p, R\}$, among all admissible internal processes, the one described by the parametrization that minimizes the functional $\dot{\Psi}$ is the effective one

$$\inf_{\dot{R}\in\mathbb{R}_+, \boldsymbol{N}\in\mathcal{N}} \dot{\Psi} = \frac{d}{dt} W(\boldsymbol{F}, \boldsymbol{F}^p) + \phi\left(R, \dot{R}\right) \tag{9}$$

Through the optimality conditions, one can arrive at the desired equations

$$\boldsymbol{N} = \frac{1}{\sqrt{2}} \frac{\mathrm{dev}^s(\boldsymbol{M}^e)}{\mathrm{dev}^s(\boldsymbol{M}^e)} \tag{10}$$

$$-\frac{1}{\sqrt{2}} \|\mathrm{dev}^s(\boldsymbol{M}^e)\| + s(R)\dot{R}^m = 0 \tag{11}$$

where $\boldsymbol{M}^e$ is the Mandel stress, and $\mathrm{dev}^s(\cdot)$ stands for the symmetric-deviatoric operator. This way the evolution of the internal variables $\dot{\boldsymbol{F}}^p$ (eq. 8) and $\dot{R}$ is completely defined, analogously to the model presented by [2].

Following the variational framework [6], the first Piola-Kirchhoff stress tensor can be obtained directly from the effective potential Ψ^{eff}

$$\dot{\Psi}^{eff}\left(\dot{\boldsymbol{F}}\right) = \inf_{\dot{R}\in\mathbb{R}_+, \boldsymbol{N}\in\mathcal{N}} \dot{\Psi} = \frac{d}{dt}\psi(\boldsymbol{F}, \boldsymbol{F}^p) + \phi\left(R, \dot{R}\right) \tag{12}$$

through the operation

$$\boldsymbol{P} = \frac{\partial}{\partial \dot{\boldsymbol{F}}} \Psi^{eff}\left(\dot{\boldsymbol{F}}\right) \tag{13}$$

Straightforwardly, the Cauchy stress can be obtained from $\boldsymbol{P}$ through the usual transformation

$$\boldsymbol{\sigma} = J^{-1}\boldsymbol{P}\boldsymbol{F}^T \tag{14}$$

which renders 3 additive terms, each one derived from the corresponding energetic potential,

$$\boldsymbol{\sigma} = \boldsymbol{\sigma}_{vol} + \boldsymbol{\sigma}_{ec} + \boldsymbol{\sigma}_m. \tag{15}$$

2.4 Incremental Constitutive Update

The incremental version of the variational problem (9) is approached in details in reference [6]. It can be stated as follows:

Incremental Variational Update Given a state $\mathcal{E}_n$ at time t_n and the total deformation gradient $\boldsymbol{F}_{n+1}$ at time t_{n+1}, among all admissible updated states $\mathcal{E}_{n+1}$ at time t_{n+1}, the one described by the parametrization that minimizes the incremental functional Ψ_{inc} corresponds to the effective updated state

$$\inf_{\mathring{R}\in\mathbb{R}_+, \boldsymbol{N}\in\mathcal{N}} \Psi_{inc} = \psi\left(\boldsymbol{F}_{n+1}, \boldsymbol{F}^p_{n+1}\right) - \psi(\boldsymbol{F}_n, \boldsymbol{F}^p_n) + \Delta t\,\phi\left(R_{n+\alpha}, \mathring{R}\right) \tag{16}$$

where $\alpha \in [0,1]$ is an algorithmic parameter analogous to an integration parameter. Some terms need to be detailed. As we are dealing with an incremental version of the constitutive problem, the rate $\dot{R}$ and the relation (8) must be somehow rewritten by their discrete counterparts. The discrete version of $\dot{R}$ becomes $\mathring{R}$ and keeps the same physical meaning as before, relating the states R_{n+1} and R_n by

$$R_{n+1} = R_n + \Delta t\mathring{R} \tag{17}$$

The inelastic deformation gradient update $\boldsymbol{F}^p_{n+1}$ is performed by means of the exponential mapping [18]

$$\boldsymbol{F}^p_{n+1} = \mathrm{EXP}\left[\Delta t\,\boldsymbol{D}^p\right]\boldsymbol{F}^p_n \tag{18}$$

due to its property of preserving the value of the determinant $\det \boldsymbol{F}^p_{n+1} = \det \boldsymbol{F}^p_n = 1$ if the traceless condition $\mathrm{tr}\boldsymbol{D}^p = 0$ is fulfilled, without imposing any additional constraint to the problem. The optimality condition of (16) provides an analytical flow direction $\boldsymbol{N}$ given by

$$\boldsymbol{N} = \frac{1}{\sqrt{2}} \frac{\operatorname{dev}\left(\boldsymbol{\varepsilon}_{n+1}^{pre}\right)}{\left\|\operatorname{dev}\left(\boldsymbol{\varepsilon}_{n+1}^{pre}\right)\right\|} \tag{19}$$

which depends solely on an elastic predictor state [10]. That is, an elastic predictor state is a fictitious state defined at time t_{n+1} in which kinematic variables associated to inelastic quantities are held fixed at the previous time t_n. Therefore the elastic deformation gradient associated to the predictor state is given by $\boldsymbol{F}_{n+1}^{pre} = \boldsymbol{F}_{n+1}^{iso} \boldsymbol{F}_n^{p-1}$, conjointly with the right Cauchy-Green tensor $\boldsymbol{C}_{n+1}^{pre} = \left[\boldsymbol{F}_{n+1}^{pre}\right]^T \boldsymbol{F}_{n+1}^{pre}$, and the elastic predictor logarithmic strain $\boldsymbol{\varepsilon}^{pre} = \frac{1}{2} \ln \boldsymbol{C}^{pre}$. The single equation to be solved that arises from the optimality condition is thus

$$\mathring{R} - \frac{\sqrt{2}}{\Delta t} \left\|\operatorname{dev}\left(\boldsymbol{\varepsilon}_{n+1}^{pre}\right)\right\| + \frac{s\left(R_{n+\alpha}\right)}{G\Delta t} \mathring{R}^m + \frac{\alpha}{G} \frac{ds}{dR}\left(R_{n+\alpha}\right) \frac{\mathring{R}^{m+1}}{m+1} = 0 \tag{20}$$

After solving it, the variables $\mathring{R}$ and $\boldsymbol{N}$ (19) are used to update states $(\mathcal{E}_n \rightarrow \mathcal{E}_{n+1})$ (eqs. 18 and 17). Analogously to the continuum time formulation (9), the first Piola-Kirchhoff is obtained directly from the effective incremental potential [6]

$$\Psi_{inc}^{eff}\left(\boldsymbol{F}_{n+1}\right) = \inf_{\mathring{R}\in\mathbb{R}_+, \boldsymbol{N}\in\mathcal{N}} \psi\left(\boldsymbol{F}_{n+1}, \boldsymbol{F}_{n+1}^p\right) - \psi\left(\boldsymbol{F}_n, \boldsymbol{F}_n^p\right) + \Delta t \phi\left(R_{n+\alpha}, \mathring{R}\right)$$

by its differentiation

$$\boldsymbol{P}_{n+1} = \frac{\partial \Psi_{inc}^{eff}}{\partial \boldsymbol{F}_{n+1}} \tag{21}$$

which ends up generating the same relations for the updated Cauchy stress $\boldsymbol{\sigma}_{n+1}$ (15), but all the quantities being evaluated at the updated state $\mathcal{E}_{n+1}$.

3 Numerical Results

3.1 Model Assessment

The main purpose of this section is to address some numerical experimentations with the proposed model in order to verify its capabilities. Therefore, we do not intend to provide, nor claim to have found, any useful material parameter to be used in real applications, due to the small number of experiments used to calibrate the model.

In order to completely define the model, 10 material parameters are required; the set $\{m, s_0, s_\infty, \zeta, \beta, \gamma\}$ defines the dissipative potential (4) and the flow resistance (6), $\{G\}$ defines the quadratic Hencky potential , $\{\lambda_{lock}, \mu\}$ defines the eight-chain hyperelastic model, $\{\kappa\}$ is related to volumetric effects. Some experimental results for a sample of poly(methyl methacrylate) (PMMA) are available in the work of [8]. These authors performed some compression tests at different strain rates $\left\{10^{-1}, 10^{-2}, 10^{-3}, 3(10^{-4})\right\}$ $[1/s]$, and along with the fitting results, can be visualized in figure (2). In fig. (2a) the stress-strain curve is presented, where the markers refer to experimental data (obtained from [8]) and the continuum lines are the predicted response of our model. Note the agreement between both the experimental and the numerical results. The figure (2b) depicts the associated flow resistance (eq. 6) and its evolution. A loss of 40% of resistance in relation to the initial resistance can be verified.

Another set of experimental results was extracted from the work of [7]. In this case, loading-unloading compression tests were performed with polycarbonate (PC) at different unloading strains. The figure (3a) shows the stress-strain curves that were obtained, where again the markers are the experimental data and the continuum lines refer to the model prediction. The initial aspects of the stress-strain, capturing the strain softening phenomena and the post-yielding hardening, could be well described, however the unloading aspects of the curve were only satisfactory. The flow resistance associated to this material can be checked in figure (3b), where a loss of 40% of resistance could be found as well, if compared against the initial state.

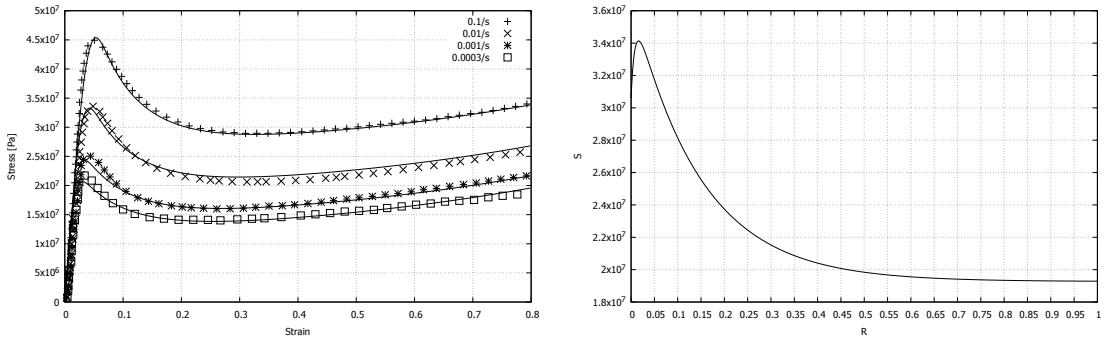

(a) Stress x Strain Curves (b) Flow Resistance

Figure 2: PMMA. Experimental results from [8] (markers) and fitted model (solid lines).

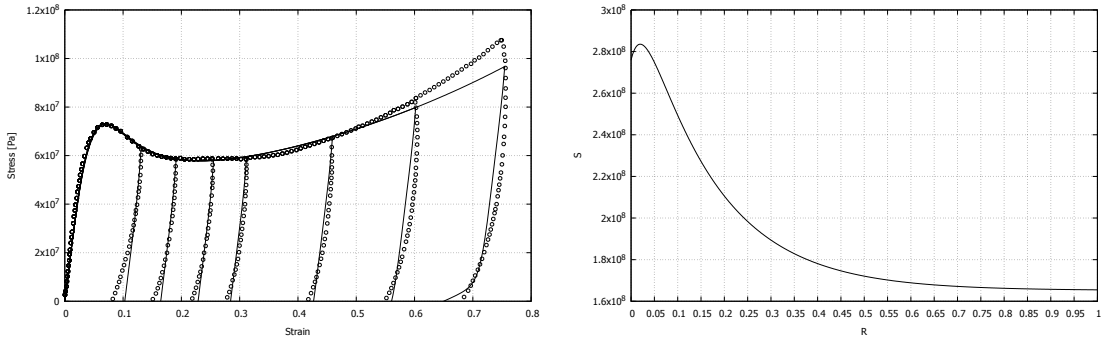

(a) Stress x Strain Curves (b) Flow Resistance

Figure 3: PC Experimental results from [7] (markers) and fitted model (solid lines).

3.2 Convergence

Being a numerical framework and based on time discrete approximations, it becomes important to verify how time intervals influence the solution specially concerning stress convergence and the overall shape of stress-strain curves. In order to check convergence, different simulations were performed, each one having its own time interval (Δt) and integration parameter (α) (see 16). A reference solution was obtained using a large number of time divisions, namely $3 \cdot 10^5$ divisions , thus resulting in a small time interval. Figure (4a) gathers all these results. As the time interval reduces, so does the maximum relative error in stress given by $\max_{t \in [t_0, t_f]} \frac{\|\boldsymbol{\sigma} - \boldsymbol{\sigma}_{ref}\|}{\|\boldsymbol{\sigma}_{ref}\|}$. For small time intervals a linear convergence was observed, which matches the observations of [9] for small strain J2 plasticity and is consistent with a backward-Euler scheme . One can see that for these experiments, an integration parameter of $\alpha = 0.5$ performed the best, although as pointed out by [9] there may actually be another optimal α parameter. The stress-strain curve is presented in figure (4b) for a different number of time divisions $ndiv \in \left\{2^i \cdot 10, i = 1, 12\right\}$ and for the integration parameter $\alpha = 0.5$. It can be noted that the overall curve shape converges relatively fast, apparently from below, and did not show any evidence of an oscillating convergence.

3.3 Tensile Test

The proposed viscoelastic model was implemented inside a FEM framework to verify its performance. A simple tensile test of a 3D specimen was performed using the fitted PMMA material (fig. 2a). Due to symmetries, only one-eighth of the structure was discretized, rendering a model with a coarse mesh of 500 8-noded brick elements and 2754 degrees of freedom. A prescribed displacement was set at the top and symmetry boundary conditions were applied at the corresponding faces. The converge was smooth with an average of 4 global newton iterations per time step. The deformed (unscaled) mesh is shown in figure (5a) at the end of the simulation.

The axial Cauchy stress evolution was analyzed at the 6 elements depicted in figure (5a) and the

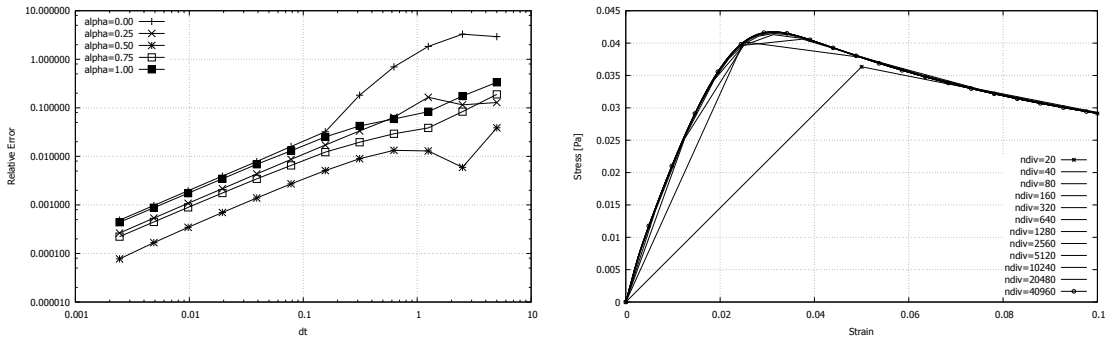

(a) Maximum relative error

(b) Stress-Strain Curve Convergence

Figure 4: Convergence assessments

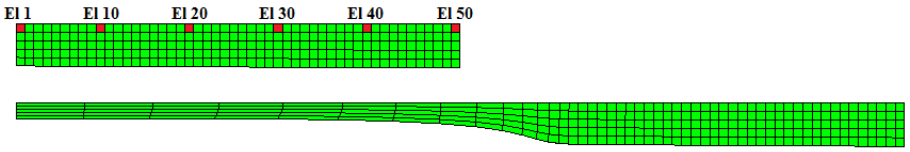

(a) Initial mesh and unscaled deformed mesh at $t = 10s$

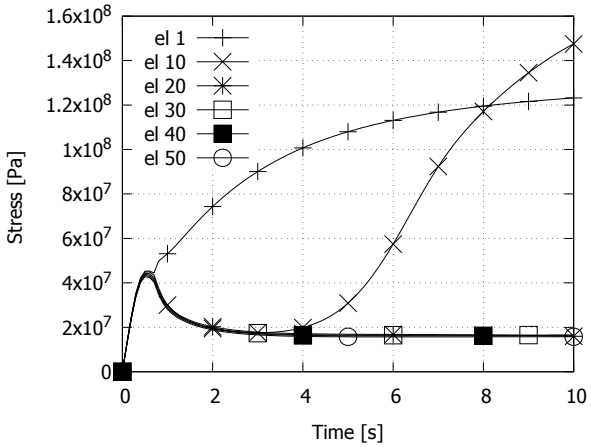

(b) Stress Evolution

Figure 5: Example of a FEM simulation

results presented in figure (5b). It is interesting to note how different sections of the geometry are solicited during the deformation process, as each one undergoes a softening phenomenon followed by a recovery of resistance.

4 Conclusions

An alternative thermodynamic formulation has been developed for predicting the behavior of glassy polymers. It is based on the concept of a flow resistance state dependent variable, instead of internal variables as is commonly adopted in the literature. An explicit flow resistance function is proposed, which increases the model's versatility and makes it easier to understand the softening nature of these class of polymers, allowing the recovery of other models and behaviors, such as Newtonian viscous flow, Perzyna flow, BPA model. Numerical assessments of the model showed an excellent agreement with simple compression experiments, and a monotonic stress convergence could be observed for smaller time steps. A FEM framework was used to verify a tensile test in a 3D specimen, and the algorithm's performance was based uniquely on the solution of a single scalar equation at each integration point, which renders a computationally robust algorithm.

References

[1] L. Anand , N.M. Ames. *On modeling the micro-indentation response of an amorphous polymer,* International Journal of Plasticity 22 , 1123–1170 , 2006.

[2] L. Anand, M. E. Gurtin. *A theory of amorphous solids undergoing large deformations, with application to polymeric glasses,* International Journal of Solids and Structures 40 , 1465–1487 , 2003.

[3] M. C. Boyce, D. M. Parks, A. S. Argon. *Large inelastic deformation of glassy polymers. Part I: Rate Dependent constitutive model*, Mechanics of Materials 7 , 15 - 33 , 1988 .

[4] R. N. Haward, G. Thackray. *The Use of a Mathematical Model to Describe Isothermal Stress-Strain Curves in Glassy Thermoplastics,* Proc. R. Soc. Lond. A 302, 453-472, 1968.

[5] S. Holopainen. *Modeling of the mechanical behavior of amorphous glassy polymers under variable loadings and comparison with state-of-the-art model predictions*, Mechanics of Materials 66 , 35 - 58 , 2013.

[6] M. Ortiz, L. Stainier. *The variational formulation of viscoplastic constitutive updates*, Computer methods in applied mechanics and engineering 171, 419 - 444 , 1999.

[7] C. Dreistadt, et al. *Experimental study of the polycarbonate behaviour during complex loadings and comparison with the Boyce, Parks and Argon model predictions,* Materials and Design 30 , 3126–3140 , 2009.

[8] N. M. Ames, et al. *A thermo-mechanically coupled theory for large deformations of amorphous polymers. Part II: Applications.* International Journal of Plasticity 25, 1495–1539, 2009.

[9] L. Brassart , L. Stainier. On convergence properties of variational constitutive updates for elasto-viscoplasticity, GAMM-Mitteilungen 35, 26 - 42, 2012.

[10] E.A. Fancello, J.-P. Ponthot, L. Stainier. *A variational formulation of constitutive models and updates in non-linear finite viscoelasticity*. International Journal for Numerical Methods in Engineering 65, 1831-1864, 2006.

[11] E.A. Fancello, J.P. Ponthot, L. Stainier. *A variational framework for nonlinear viscoelastic models in finite deformation regime.* Journal of Computational and Applied Mathematics 215 , 400–408 , 2008.

[12] E. Fancello, J. M. Vassoler, L. Stainier. *A variational constitutive update algorithm for a set of isotropic hyperelastic–viscoplastic material models*, Comput. Methods Appl. Mech. Engrg. 197 , 4132–4148 , 2008.

[13] Q. Yang, L. Stainier, M. Ortiz. *A variational formulation of the coupled thermo-mechanical boundary-value problem for general dissipative solids*, Journal of the Mechanics and Physics of Solids 54 , 401–424 , 2006.

[14] C. Nakafuku, S.-y. Takehisa. *Glass Transition and Mechanical Properties of PLLA and PDLLA-PGA Copolymer Blends*. Journal of Applied Polymer Science 93, 2164-2173, 2004.

[15] W. A. Spitzig, O. Richmond. *Effect of hydrostatic pressure on the deformation behavior of polyethylene and polycarbonate in tension and in compression*. Polymer Engineering and Science 19, p. 1129–1139, 1979.

[16] J.C. Simo, R.L. Taylor. *Quasi incompressible finite elasticity in principal stretches continuum basis and numerical algorithms*. Computer Methods in Applied Mechanics and Engineering 85, 273–310, 1991.

[17] E. M. Arruda, M. C. Boyce. *A three-dimensional constitutive model for the large stretch behavior of rubber elastic materials*. J. Mech. Phys. Solids 41, 389-412 , 1993.

[18] G. Weber , L. Anand. *Finite deformation constitutive equations and a time integration procedure for isotropic, hyperelastic-viscoplastic solids*. Computer Methods in Applied Mechanics and Engineering 79, 173-202 , 1990.

[19] J.C. Simo, R.L. Taylor , K.S. Pister, *Variational and projection methods for the volume constraint in finite deformation elasto-plasticity*. Computer Methods in Applied Mechanics and Engineering 51, 177-208 , 1985.